ACS APPLIED MATERIALS & INTERFACES

RESEARCH ARTICLE

www.acsami.org

Direct Grafting of Long-Lived Luminescent Indicator Dyes to GaN Light-Emitting Diodes for Chemical Microsensor Development

Juan López-Gejo,[†] Álvaro Navarro-Tobar,[‡] Antonio Arranz,[§] Carlos Palacio,[§] Elías Muñoz,[‡] and Guillermo Orellana*[,†]

[†]Department of Organic Chemistry, Faculty of Chemistry, Universidad Complutense de Madrid, 28040 Madrid, Spain

[‡]ISOM and Department of Electronic Engineering, ETSI Telecomunicación, Universidad Politécnica de Madrid, 28040 Madrid, Spain

[§]Department of Applied Physics, Faculty of Science, Módulo 12, Universidad Autónoma de Madrid, Cantoblanco, 28049 Madrid, Spain

Supporting Information

ABSTRACT: Two new methods for covalent functionalization of GaN based on plasma activation of its surface are presented. Both of them allow attachment of sulfonated luminescent ruthenium(II) indicator dyes to the p- and n-type semiconductor as well as to the surface of nonencapsulated chips of GaN light-emitting diodes (blue LEDs). X-ray photoelectron spectroscopy analysis of the functionalized semiconductor confirms the formation of covalent bonds between the GaN surface and the dye. Confocal fluorescence microscopy with single-photon-timing (SPT) detection has been used for characterization of the functionalized surfaces and LED chips. While the ruthenium complex attached to p-GaN under an oxygen-free atmosphere gives significantly long mean emission lifetimes for the indicator dye (ca. 2000 ns), the n-GaN-functionalized surfaces display surprisingly low values (600 ns), suggesting the occurrence of a quenching process. A photoinduced electron injection from the dye to the semiconductor conduction band, followed by a fast back electron transfer, is proposed to be responsible for the excited ruthenium dye deactivation. This process invalidates the use of the n-GaN/dye system for sensing applications. However, for p-GaN/dye materials, the luminescence decay accelerates in the presence of O_2. The moderate sensitivity is attributed to the fact that only a monolayer of indicator dye is anchored to the semiconductor surface but serves as a demonstrator device. Moreover, the luminescence decays of the functionalized LED chip measured with excitation of either an external (laser) source or the underlying LED emission (from p-GaN/InGaN quantum wells) yield the same mean luminescence lifetime. These results pave the way for using advanced LEDs to develop integrateable optochemical microsensors for gas analysis.

KEYWORDS: optical chemical microsensors, GaN LED, surface grafting, luminescence lifetime, ruthenium indicator dye

1. INTRODUCTION

The *cell-phone-as-a-sensor* concept has gained attention for many applications that span from national and personal security to individual healthcare.[1] For instance, smart cell phones and inexpensive, commonly available sensor devices could create an opportunity to reach people who previously had no access to technology-based healthcare solutions.[2,3] At the same time, the huge number of circulating cell phones might provide a unique (bio)sensing network for monitoring hazardous chemical emissions, bacterial aerosols, or explosives manipulation, to name a few.[4] To take advantage of those scenarios, cell phones must incorporate specific microchemo-(bio)sensors for detecting the target analyte for each application. Among the different sensor types, optical chemical sensors display several advantages, including the lack of analyte consumption, specificity, robustness, and possibility of contactless measurements.[5] Nevertheless, miniaturization of the optical block [a dedicated light-emitting diode (LED) as the excitation source, an optochemical transducer, and photodetector elements] required by sensor integration into a cell phone or a hand-held monitor is not a trivial issue.

Recently, an emission-lifetime-based micro*fluorometer* has been built with an Al−In−Ga−N LED as the excitation source and a vertically opposed 16 × 4 array of single-photon avalanche diodes fabricated in 0.35-μm high-voltage CMOS technology with in-pixel time-gated photon-counting circuitry.[6] The array is capable of producing 777-ps (full width at half-maximum) sample excitation pulses, enabling short-emission-lifetime fluorophores to be monitored. Within a similar microdevice, surface functionalization of the light-emitting semiconductors with tailored luminescent molecular probes would provide integrated microcircuits with gas-sensing features. Luminescence-lifetime-based sensors display the highest stability compared to intensity-based devices because they are insensitive to indicator photobleaching, light-source fluctuations, and detector aging. Moreover, for sensing applications, a system based on the frequency domain rather than pulse-probe detection (namely, luminescence phase shift determination by the demodulation technique, similar to that currently used in mobile telephony) is usually the selected choice in commercial instrumentation.[7] In this case, the excited-state lifetime of the

Received: May 11, 2011
Accepted: September 26, 2011
Published: September 26, 2011

luminescent dye is calculated from the phase shift between a sinusoidally modulated excitation wave and the modulated emission wave. All of these processes and control functions would be readily performed with current smartphones. Therefore, we have tackled in our work the ultraminiaturization of the optical block.

In a previous communication, we described for the first time the covalent functionalization of GaN surfaces with an oxygen-sensitive ruthenium dye complex, as a proof-of-concept toward new microsensing devices.[8,9] The advantage behind such functionalization is to use the semiconductor not only as a substrate of the luminescent dye but also as the excitation source, bringing an optical chemosensor down to the microscale. In modern semiconductor-based LED structures, total internal reflection due to the high refractive index of the material ($n_{GaN,460\ nm}$ = 2.42) and reabsorption of light limits extraction of light, and, consequently, the overall efficiency of a LED light source.[10] Anchoring the luminescent indicator dye directly to the GaN surface guarantees a highly efficient excitation.

Nitride semiconductors possess exceptional physical, electronic, and optoelectronic properties, such as physical hardness, chemical stability, high electron mobility, large critical breakdown field, significant thermal conductivity, and wide band gap, allowing their current use in many applications such as illumination, data storage, and high-speed/high-power electronics.[11] Adsorption,[12−15] deposition,[16−18] and covalent binding have all been proven to be valid functionalization methods of GaN surfaces. Among them, chemical functionalization of the semiconductor surface is arguably the most interesting one for sensing applications because of the outstanding stability of the resulting interface. Thus, the covalent attachment of alkenes,[19,20] phosphonic acids,[21] mercaptosilanes[22−24] or aminosilanes[8,9,24−28] to GaN surfaces has successfully been achieved and eventually used to tether more complex molecules such as DNA,[13−15,19,20,22,26] proteins,[16,26] or zeolites[27] for various electronic, photonic, biomedical, and sensing applications. Moreover, in addition to simple surfaces, GaN nanowires[16,22,26,29,30] and GaN quantum dots[31] with high surface-to-volume ratios have also been derivatized.

Luminescent ruthenium(II) polyazaheterocyclic complexes pervade among the O_2 indicator dyes for environmental and industrial applications because of their wide absorption in the blue region, strong red emission, 0.2−8 μs luminescence lifetimes, high photostability, and the near-diffusion-limited O_2 quenching rate of their metal-to-ligand charge-transfer (^{3}MLCT) excited state.[32] Most importantly, the analyte-tunable ligands also allow the design of different chemical methods for covalent grafting of the ruthenium(II) luminescent dyes to many types of surfaces such as semiconductors, glass, metals, or graphite.[33−36] Capitalizing on the strength and versatility of the amide chemical bond, two novel functionalization methods are described in this work that allow derivatization of LED chips without disturbance of the emission features of such devices for sensing applications. Using plasma activation of the semiconductor, a sulfonic acid derivative of tris(4,7-diphenyl)-1,10-phenanthroline has been chemically attached to both n- and p-type GaN wafer dices and standard GaN blue LEDs.

2. EXPERIMENTAL SECTION

2.1. Functionalization of the GaN Surfaces. About 7 × 7 mm samples of n-type GaN were cut from a commercial substrate (wafers from Lumilog, Vallauris, France), while p-type GaN samples (7 × 7 mm) were grown over sapphire substrates by metal−organic molecular beam epitaxy and activated for 25 min at 800 °C in a rapid-thermal-annealing oven. The nominal acceptor concentration is 1 × 10^{19} cm^{-3}. Standard GaN blue LED having GaN/InGaN quantum wells (BL470A, 300 × 300 μm) were supplied by FOREPI-Formosa Epitaxy (Lung-Tan, Taoyuan, Taiwan; Figure S4 in the Supporting Information). For the first functionalization method, an oxygen plasma treatment was applied for 10 min (O_2 flow = 7 sccm; radio-frequency applied power = 93 W; pressure = 60 mTorr; time = 10 min; direct-current bias measured under those conditions = 300 V). After the oxygen plasma treatment, each sample was introduced in 7 mL of a 20 mM (3-aminopropyl)triethoxysilane (APTES) solution for 12 h. Following silanization, all samples were exhaustively washed with toluene. For the second functionalization method of the semiconductor, a microwave air plasma (800 W, 1−2 mbar) was applied for 15 min. The air was previously saturated by bubbling through water at the entrance of the plasma chamber. The synthesis of the starting dye molecule, tetrasodium tris[(1,10-phenanthroline-4,7-diyl)bis(benzenesulfonate)]-ruthenate(4−) (abbreviated $Na_4[Ru(pbbs)_3]$), has been described elsewhere.[40] The corresponding sulfonyl chloride of the ruthenium complex was synthesized by refluxing $Na_4[Ru(pbbs)_3]$ (4 mg) in $SOCl_2$ (2 mL, Fluka) containing 5 drops of dimethylformamide (DMF; ≥99.8%, Fluka) for 3 h. The excess of $SOCl_2$ was removed by vacuum distillation at ca. 50 °C, and the solid red-orange product was dissolved in 5 mL of DMF. The silanized GaN surfaces were introduced into a glass vial, and 2 mL of the latter solution was added together with 3 drops of *N*,*N*-diisopropylethylamine (Sigma-Aldrich). The mixture was then stirred at room temperature for 48 h, leading to the formation of the corresponding sulfonamide upon the reaction of sulfonyl chloride of the indicator dye with alkylamine tethered to the GaN surface. Finally, the functionalized surface was thoroughly washed with analytical- or high-performance liquid chromatography (HPLC)-grade DMF, acetone, methanol, purified water (18 MΩ cm, Millipore Direct-Q), and acetone. Samples were subsequently dried under air. In the course of our preliminary studies for optimizing the dye attachment, no luminescence decay could be observed at all after the washing process when a functionalization reaction did not work. Following chemical functionalization, the LED electrical contacts were welded in order to apply the electrical current and operate the device. Glass samples (7 × 7 mm) were cut from a microscope slide and functionalized following the same procedure as that for the GaN samples, with the only difference being that silanol activation was performed chemically with a "piranha" solution (4 mL of H_2SO_4 and 2 mL of H_2O_2) for 20 min instead of plasma treatment.

2.2. Luminescence Decay Measurements. A Horiba (Piscataway, NJ) DynaMic fluorescence lifetime imaging microscope (FLIM) was used to characterize the functionalized LED chips and GaN wafers. The system includes an epifluorescence confocal microscope (Olympus BX51) equipped with 10× and 40× objectives, a 1600 × 1200 pixel CCD camera (uEye UI-1450-C; IDS, Cologne, Germany) for bright-field image recording, and a 1392 × 1040 pixel INFINITY3-1C cooled color CCD camera (Lumenera Corp., Ottawa, Ontario, Canada) for fluorescence imaging (Scheme S1 in the Supporting Information). A laser diode (Horiba NanoLED-470LH) was used as the external excitation source (463 nm peak wavelength; 900 ps pulse width; 100, 50, or 10 kHz repetition rate). A 470-nm interference filter (Chroma HQ470/20x, Rockingham, VT) was intercalated in the excitation path, and a 490-nm dichroic mirror (Olympus Q490DCXR) was placed in the 6-position cube turret. Because the emission maximum of the investigated samples was around 630 nm, a 590-nm cutoff filter (CG-OG-590-1.00-3; CVI Technical Optics, Onchan Isle of Man, U.K.) was used to minimize the detection of scattered light in the emission beam. The Horiba FluoroHub controller for sequential single-photon-timing (SPT) detection was interfaced to a Horiba TBX-04D picosecond photon detection module equipped with a fast red-sensitive photomultiplier tube (PMT) detector with thermoelectric cooling for lower noise operation. Variable delay times with respect to the trigger pulse could be adjusted with an external gate and delay generator (Ortec 416A, Atlanta, GA). Luminescence decays were measured with a 10 or 20 μs window by accumulating the signal over at least 5000 counts in the

Scheme 1. Preparation of the Luminescent Ru(pbbs)$_3$-Grafted GaN Surface Using (a) an O_2 Plasma or (b) Direct Amination with a Humid-Air Plasma[a]

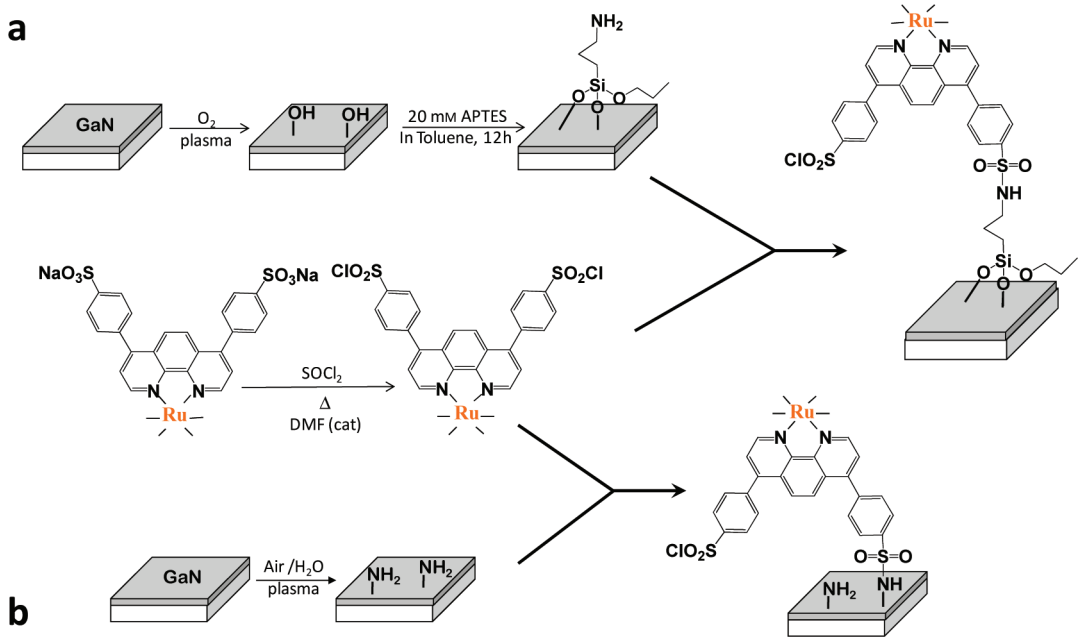

[a] Both procedures end with aminoalkyl silanization followed by the formation of a sulfonamide.

peak channel. Preexponentially weighted mean emission lifetimes[37] were obtained thereof after triexponential curve fittings using the proprietary Horiba hybrid grid-search minimization algorithm (without deconvolution) for stable χ^2 minimization. The reduced χ_r^2 (<1.1), weighted residuals, and autocorrelation functions were employed to judge the goodness of the fits. Measurements were carried out under atmospheric pressure (711 ± 5 Torr). Unlike the blue LEDs, the blue laser diode used in the FLIM measurements is linearly polarized. To check for any artifact or effect of the polarized excitation on the ruthenium indicator dye emission decay, luminescence lifetime measurements on a functionalized p-GaN sample using a state-of-the-art SPT fluorometer (Horiba Fluoromax-4SPT) were performed. Three different excitation sources, pulsed at 10 kHz, were used on the *same* sample spot by placing it within the Horiba 1933 solid-sample-holder accessory: the 463-nm laser diode (see above), a 450-nm LED (Horiba NanoLED-450, 1.1-ns pulse width), and a 405-nm laser diode (Horiba NanoLED-405LH, <700-ps pulse width). The preexponentially weighted emission lifetimes extracted from the respective decay curves (see Figure S1 in the Supporting Information) showed no significant differences, therefore excluding the existence of any photoselection effect.

For interrogation of the GaN LEDs, the trigger signal of the FluoroHub is fed to a pulse generator (HP8116A; Hewlett-Packard, Boeblingen, Germany). The input and output signals of the latter were monitored with an oscilloscope (TDS 2024B; Tektronix, Beaverton, OR). The synchronized signal is applied to the LED through its metal contacts (Scheme S1 in the Supporting Information), and the luminescence decay is recorded with the PMT of the FLIM equipment. The best pulse voltage, pulse width, and repetition frequency to minimize the residual red emission of the LED were found to be 3.5 V, 20−30 ns, and 100 kHz, respectively. The applied base bias voltage was −8 V, which produced an optimal fall time for the LED emission. In order to optimize the temporal response of the excitation source and avoid reflections due to impedance mismatch, the pulse generator was set to 50 Ω coupling and the transmission line was terminated with a 50 Ω parallel resistor close to the LED.

2.3. X-ray Photoelectron Spectroscopy (XPS) Measurements. The XPS analysis was performed in an ultrahigh-vacuum system at a base pressure better than 6×10^{-10} Torr. XPS spectra were measured using a hemispherical analyzer (SPECS Phoibos 100 MCD-5). The pass energy was 9 eV, giving a constant resolution of 0.9 eV. The Au $4f_{7/2}$, Ag $3d_{5/2}$, and Cu $2p_{3/2}$ lines of reference samples at 84.0, 368.3, and 932.7 eV, respectively, were used to calibrate binding energies. Although sample charging was observed because of the insulating character of the sapphire substrates on which GaN layers were grown, this effect was corrected, peaking the C 1s band at 285.0 eV and shifting accordingly all other core levels. A twin-anode (Mg/Al) X-ray source was operated at a constant power of 300 W. The S 2p and C 1s core level spectra were recorded using Al Kα radiation to avoid the strong overlapping of those photoemission peaks with the Ga LMM Auger transition.

3. RESULTS AND DISCUSSION

3.1. Functionalization and Characterization of Chemosensitive GaN. The method known so far for grafting ruthenium(II) complexes to GaN surfaces requires three steps:[8,9] (i) oxidation of the material outermost layer; (ii) aminosilanization of the hydroxylated surface, and (iii) covalent attachment of the polysulfonated ruthenium indicator dye. The oxidation step is performed by introducing the semiconductor to a H_2SO_4/H_2O_2 ("piranha") mixture for 30−60 min. Such a chemical oxidation turned out to be too aggressive for the metal−semiconductor contacts of the LED chip, and after chemical oxidation, the LED became totally inoperative. Therefore, two new methods based on plasma treatment (Scheme 1) have been developed as an alternative for the semiconductor device functionalization. Both methods have been tested initially on n- and p-type GaN samples and characterized with XPS and SPT luminescence measurements.

For the first method (method a, Scheme 1), an oxygen plasma was used to generate hydroxyl groups on the GaN surfaces. After the plasma treatment, a silanization process was carried out with

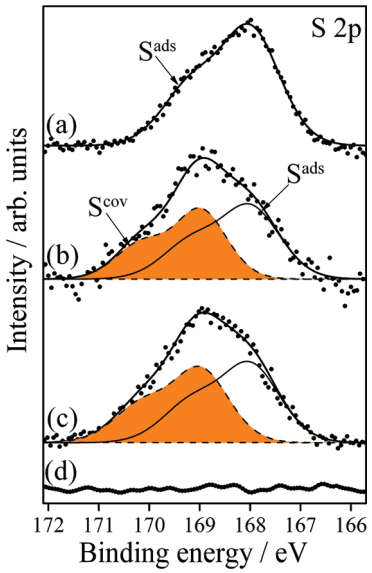

Figure 1. S 2p core level XPS spectra (dots) and corresponding best-fit curves (thick solid lines) of $[Ru(pbbs)_3]^{4-}$ on n-GaN surfaces for (a) the adsorbed dye, (b) the dye bound after chemical oxidation of the semiconductor surface, (c) the dye bound after oxygen plasma oxidation of the semiconductor surface, and (d) the dye bound after humid-air plasma amination of the semiconductor surface. Deconvolution of spectra b and c yields information on the sulfonamide (shadowed area) and sulfonate (nonshadowed area) groups of the covalently bonded ruthenium indicator dye.

APTES to introduce interfacial amino groups. Once the surface is aminated, the luminescent dye becomes covalently attached to the semiconductor by the formation of a sulfonamide bond after reaction of the surface amino groups with the sulfonyl chloride derivative of the ruthenium indicator. An alternative and potentially simpler method (method b, Scheme 1) is the treatment of the semiconductor surface with a humid-air plasma. According to Stein et al., amino groups are generated in this way directly on GaN surfaces after such a treatment,[38] so that no silanization is required to introduce the amino groups and the entire functionalization procedure is reduced to two steps. After humid-air plasma treatment, the ruthenium dye would anchor to the semiconductor surface by formation of the corresponding sulfonamide.

Characterization of the samples after the plasma treatments was performed by XPS and SPT. Figure 1 shows the S 2p core level XPS spectra of the n-GaN samples subject to the different functionalization methods mentioned above. The spectra have been normalized to the same height and vertically shifted for the sake of comparison. The n-type semiconductor was selected for these experiments because silanization of p-GaN is less efficient[8] and, therefore, a lower degree of ruthenium complex loading is achieved as demonstrated by a very low intensity and a poor signal-to-noise ratio of the S 2p band (data not shown). The spectrum shown in Figure 1a is representative of the S 2p core level of the *adsorbed* ruthenium complex. This experimental spectrum has been fitted by a double peak in such a way that the fitted spectrum labeled as S^{ads} (continuous line) can be used as a reference of noncovalently bound sulfonate species.[9] On the contrary, when the ruthenium complex is *covalently* bonded to the GaN substrate, after either chemical (Figure 1b) or plasma (Figure 1c) oxidation, the S 2p spectrum has a more complex shape that cannot be reproduced by a double-peaked single component. The broadening and shift of the spectrum to higher binding energies suggest that, in addition to the sulfonate groups characteristic of the ruthenium complex, other sulfur species have been formed during the covalent attachment. In this way, the experimental spectra of Figure 1b,c have been deconvoluted using two double-peak components associated with the sulfonate, S^{ads} (continuous line), and sulfonamide species, S^{cov} (dashed line and shaded area), respectively, as described elsewhere.[9] For both, the chemical and oxygen plasma oxidation of the semiconductor surface, the shape of the experimental S 2p XPS spectrum, and therefore the S^{ads}/S^{cov} ratio obtained after deconvolution are very similar, indicating that the two indicator grafting methods yield a similar degree of functionalization. In particular, values of 1.2 and 1.1, for the chemical and oxygen plasma oxidation, respectively, are obtained for the S^{ads}/S^{cov} ratio, suggesting that ca. three sulfonate groups per ruthenium complex molecule are involved in the covalent bonding with the silanized GaN substrate. Such a (low) value supports the covalent bonding of the dye because larger amounts of adsorbed ruthenium complex would lead to much higher S^{ads}/S^{cov} ratios. Integration of the sulfur band yields a value of 0.6% sulfur atoms on the semiconductor surface (all atoms included except hydrogen). Therefore, an upper limit of 0.1% surface ruthenium atoms can be grossly estimated considering that each ruthenium(II) complex contains six sulfur atoms.

In the case of humid-air plasma treatment for direct amination of the surface (Figure 1d), no sulfur signal could be detected after the indicator grafting process, indicating that no GaN functionalization or a degree of grafting below the limit of detection of the XPS technique (~0.5% atomic concentration) was achieved. Reasons for the unsuccessful functionalization can be 2-fold. One of them might be the possible inefficiency of the humid-air plasma for the formation of amino groups on the semiconductor surfaces. After a nitride semiconductor (SiN and GaN) is exposed to humidified air plasma, which contains hydroxyl radicals and free hydrogen atoms among other species, the Ga−N bonds are broken in favor of the more energetically favorable Ga−O bonds, creating $Ga-NH_2$ and Ga−OH on the surface.[39] Eventually, many amino groups could be oxidized to nitroso (−NO) or even nitro ($-NO_2$) groups under the influence of the plasma, significantly decreasing the amount of ruthenium-functionalizable anchors. Unfortunately, the N 1s core level binding energies of nitroso and nitro groups are very similar to those of amino groups,[8] so that their distinction by XPS is almost impossible because of the severe overlap of the bands associated with these nitrogen species.

The second reason for the lack of functionalization might be steric hindrance for the ruthenium complex to reach the plasma-generated amino groups. Because such groups are formed directly on the semiconductor surface, the reactive luminescent dye in solution must approach the interface closer than that for the aminosilane-functionalized GaN. For a small molecule, formation of the amide bond might not be hindered, but for a large bulky dye, such as the tris(4,7-diphenyl-1,10-phenanthroline)ruthenium(II) complex, it seems to be an insurmountable obstacle.

Among all the known ruthenium polypyridyl complexes, tris-(4,7-diphenyl-1,10-phenanthroline)ruthenium(II) and its sulfonated derivative have been reported to have an emission quantum yield around 36% and a luminescence lifetime of ca. 6 μs (in the absence of O_2), which is probably the highest of all ruthenium-based indicator dyes.[41,42] Therefore, it seems to be an ideal choice as the oxygen indicator dye.[43] The luminescence decay profiles of photoexcited n-GaN samples before and after plasma functionalization with both methods are displayed in Figure 2. The emission

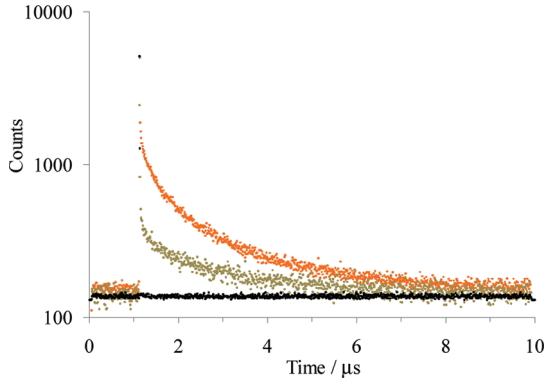

Figure 2. Luminescence decays of n-GaN before (black dots) and after covalent functionalization with the ruthenium luminescent dye using O_2 plasma (orange dots) or humid-air plasma (gray dots) (λ_{exc} = 463 nm; λ_{em} > 590 nm).

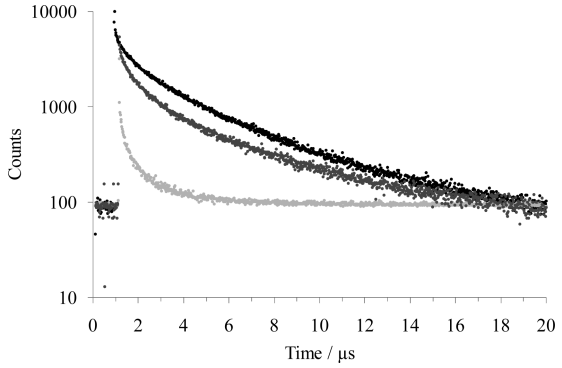

Figure 3. Luminescence decays of $Ru(pbbs)_3$-grafted n-GaN (light gray), p-GaN (black), and glass (dark gray) under argon (λ_{exc} = 463 nm; λ_{em} > 590 nm).

decay of a nonfunctionalized n-GaN sample is given for the sake of comparison, showing just the excitation light scattering.

Because SPT luminescence detection of the luminophore is a more sensitive technique than XPS, the presence of the semiconductor-grafted ruthenium complex could be detected by its red emission after any of the plasma treatments used. Nevertheless, the luminescence intensity from samples treated with method a (Scheme 1) is much more intense than that detected after functionalization method b, confirming the XPS results discussed above. The much higher efficiency of the oxygen plasma method has been observed for both n- and p-GaN samples and also for the LEDs (see below).

The SPT luminescence decays from the photoexcited $[Ru(pbbs)_3]^{4-}$ were successfully fitted without deconvolution to a sum of three exponentials. Such a multiexponential character, typical of heterogeneous systems,[43] is attributed to luminescent indicator molecules dwelling in various microenvironments with different numbers of nearby luminophores or different distances between the dye and the surface.

A comparison of the recorded emission decays of the surface-ruthenated n-GaN and p-GaN shows significant differences in their kinetics (Figure 3). While p-GaN presents a mean lifetime of ca. 2 μs under argon, the n-GaN sample displays a luminescence lifetime as low as 600 ns, pointing out the occurrence of a deactivation process involving the ruthenium(II) dye.

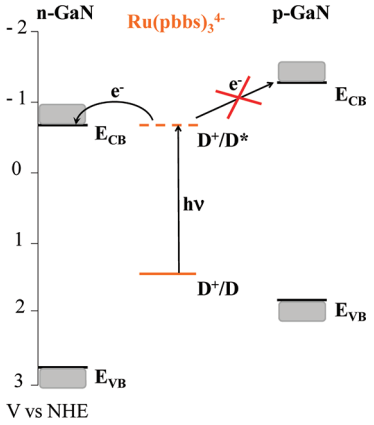

Figure 4. Scheme of the redox potentials of $[Ru(pbbs)_3]^{4-}$ and GaN and the electron-transfer process from the photoexcited metal complex to the n-type semiconductor.

Metal polypyridyls are known to participate in photoinduced electron-, energy-, and proton-transfer processes.[32,44] Proton transfer can be ruled out because of the absence of readily protonatable groups in the periphery of the ruthenium(II) coordination complex. Förster resonance energy transfer to the semiconductor cannot occur because there is no overlap between the donor emission (dye) and the acceptor absorption (GaN). Therefore, the observed excited-state quenching by n-GaN must imply a photoinduced electron transfer between the organic dye and the semiconductor. Such a photochemical process is spontaneous only if the redox potentials of the semiconductor bands and of the dye have the proper values. In fact, luminescence of the ruthenium(II) complex covalently grafted to a glass surface where no charge transfer is possible (insulator material) displays a long lifetime (1.6 μs, Figure 3). Such a mean lifetime value is similar to that measured for the dye on the p-GaN surface, confirming the absence of photoinduced electron transfer for this semiconductor. Moreover, the luminescence quenching process explains that although the ruthenium grafting efficiency is lower for the p-type semiconductor than for n-GaN, as demonstrated by XPS (see above), the emission intensity from the former is as high as ca. 7 times the luminescence from the latter (Figure S2 in the Supporting Information).

Figure 4 depicts a schematic diagram of the proposed photoinduced electron-transfer process from the grafted dye to the semiconductor. The band-edge potentials of n-GaN (E_C = −0.62 V and E_B = 2.80 V vs NHE) and p-GaN (E_C = −1.29 V and E_B = 1.85 V vs NHE in water at pH 7.0) have been published.[45] The excited-state oxidation potential (D^+/D^*) of the original ruthenium dye in acetonitrile (−0.60 V vs NHE) can be calculated from the difference between the oxidation potential of the ground-state metal complex (D^+/D = 1.41 V vs NHE)[46] and the HOMO−LUMO energy gap (2.01 eV) obtained from the dye emission maximum (618 nm).[46] Although the oxidation potential of the excited ruthenium(II) complex is similar to the reduction potential of n-GaN, yielding virtually no driving force for the proposed photoinduced electron transfer, the different solvent media where the redox potentials of the partners were measured (H_2O for the semiconductor and acetonitrile for the dye) and the fact that the unprecedented photochemical quenching from the grafted dye takes place in the absence of solvent must be taken into account. In any case, Figure 4 clearly shows the impossibility of a photoinduced electron transfer from the excited dye to/from the p-GaN semiconductor regardless of any solvent correction factor.

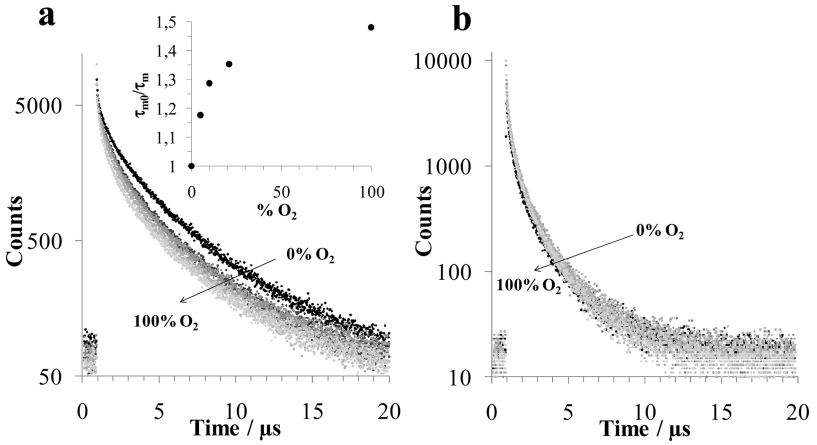

Figure 5. Evolution of the luminescence decays of ruthenium dye-grafted p-GaN (a) and n-GaN (b) with the oxygen concentration in argon (λ_{exc} = 463 nm; λ_{em} > 590 nm). Inset: Stern−Volmer plot obtained from the lifetime values in part a.

A photoinduced electron injection in octadecyltrimethoxysilane-functionalized n-GaN (but not p-GaN) has been reported recently.[47] However, in this particular case, photoexcitation was provided to the semiconductor by 254-nm UV illumination and, in this way, an electron transfer from the silane monolayer to the hole generated in the valence band of the semiconductor occurs. In our study, the dye is selectively excited with blue light, producing the electron injection to the conduction band of the GaN. To the best of our knowledge, this is the first time that a photoinduced electron injection from a dye to a nitride semiconductor is reported, paving the way also for using these materials to fabricate dye-sensitized solar cells (DSSCs).

In this regard, it must be pointed out that Chen et al. have manufactured a DSSC based on GaN functionalization with a ruthenium polypyridyl complex.[48] Nevertheless, because of the chemical stability of the semiconductor, these authors could not attach the dye directly to the semiconductor surface and had to immobilize it by absorption over a GaO or TiO_2 layer obtained by exhaustive oxidation of the GaN surface or chemical treatment with $TiCl_4$ and further oxidation. Therefore, the electronic photoinjection takes place from the adsorbed ruthenium complex to the oxide interlayer and not directly to the GaN as in our system. The covalent functionalization of GaN achieved in our work leads to a material where the dye and semiconductor are covalently bonded in close vicinity. Such a proximity may increase substantially the efficiency of the electron injection compared to dye-absorbed semiconductors.

The dye deactivation efficiency is actually so large that the functionalized n-GaN surfaces are not sensitive to the presence of O_2, as can be observed in Figure 5b. A negligible variation of the emission decay lifetime is observed when the semiconductor environment changes from 0% to 100% O_2. Therefore, it is clear that a ruthenium-functionalized n-GaN material cannot be used for sensing applications. However, in the case of p-GaN (Figure 5a), the luminescence decay accelerates and the emission lifetime notably decreases in the presence of O_2 (see also Table S1 in the Supporting Information for the emission lifetimes extracted from the multiexponential luminescence decays in Figure 5a). Although GaN displays a high affinity for O_2 adsorption on its surfaces,[49] the new functionalized material shows a moderate O_2 sensitivity (Figure 5a, inset) because of the fact that only a monolayer of the indicator dye is anchored to the surface. Nevertheless, the sensitivity of the new material is similar to that of other ruthenium

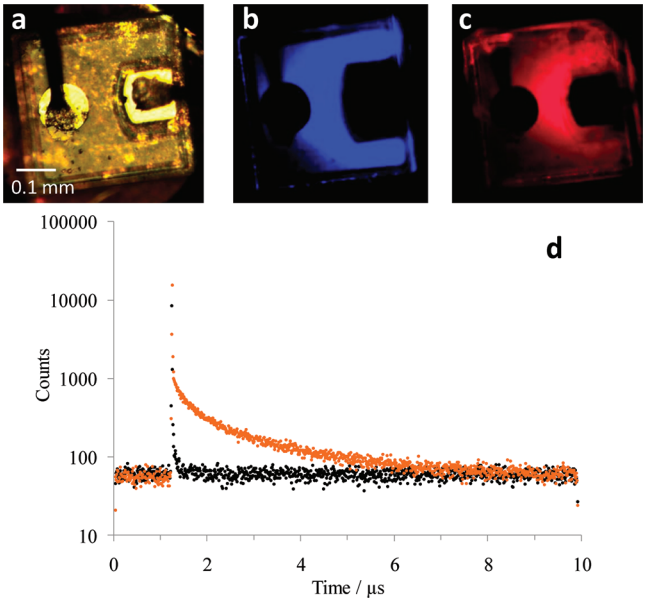

Figure 6. Microscopic images of a ruthenium dye-grafted LED: (a) bright field (50 ms exposure; gain 1.27); (b) blue emission (50 ms exposure; gain 1.27; λ_{em} > 440 nm); (c) red emission (20 s exposure; gain 6; λ_{em} > 590 nm). (d) Luminescence decays of a nonfunctionalized (black dots) and covalently functionalized LED (orange dots) in operation (λ_{em} > 590 nm).

polypyridyl-based sensors in which the indicator dye is not embedded in O_2-concentrating materials.[50,51] Encapsulating the functionalized LED surface with an O_2-permeable polymer (e.g., silicone) would boost the analyte sensitivity, as has been demonstrated for luminescent oxygen sensors.[52]

3.2. Interrogation of Ruthenium Dye-Functionalized LEDs. The two novel GaN functionalization processes, characterized by XPS and SPT luminescence measurements, have been applied to sensorization of commercial LEDs. As in the case of the GaN samples, method a (surface treatment with an oxygen plasma) is much more efficient than method b, which involves humid-air plasma activation. Figure 6 depicts the bright-field and fluorescence micrographs of a dye-grafted LED chip.

The former image (Figure 6a) gives an idea of the device size. A strong blue emission can be seen when a proper voltage is

applied to the LED (Figure 6b). Using a dichroic mirror at 490 nm and a cutoff filter at 590 nm, the red emission of the functionalized LED is also observed under the same operating conditions (Figure 6c). Nevertheless, it is well-known that GaN-based LEDs display a residual emission in the red region that peaks at ca. 670 nm.[53,54] Generally, the interference of such a residual emission on the signal from red-luminescent dyes can be eliminated using an interference filter placed between the blue LED and the sample. In our case, such a configuration is impossible because the luminescent indicator dye is grafted to the excitation source surface. Therefore, the red emission of a nonfunctionalized LED (Figure 2S) had to be minimized by optimizing its operational parameters (see the Experimental Section). Nevertheless, to confirm that the observed red emission of the functionalized LED originates from the covalently attached ruthenium complex and not from the GaN itself, the luminescence decays of an operating LED before and after the dye grafting were recorded (Figure 6d). The original device (black dots) displays only a very fast emission decay, which can be attributed to the residual red emission of the GaN, while the functionalized device (orange dots) shows also a distinct long-lived red emission characteristic of a ruthenium complex. Therefore, it can be concluded that the emission depicted in Figure 6c proceeds mainly from the tethered luminescent dye.

Finally, a comparison of the red emission decays from a functionalized device, obtained either with the external excitation (laser) source or with the internally generated blue photons by driving a current pulse through the LED chip, is depicted in Figure 7. From a visual inspection, it can be concluded that both decays are extremely similar, proving the main hypothesis that the substrate can be used as an excitation source for the development of new sensing microdevices. The only difference is the small time shift of the emission decay of the grafted dye obtained with the LED itself due to the wider pulse of the latter compared to that of the external picosecond laser diode (21 and 0.9 ns, respectively). In this regard, the long luminescence lifetime of the ruthenium(II) polypyridyl complexes facilitates their use as indicator probes for lifetime-based sensing[32] interrogated by underlying GaN diodes. Remarkably, the fit of each decay to a triexponential function yields the same mean emission lifetime (ca. 400 ns) regardless the excitation source (Table 1). Normal operation of the functionalized LED by application of the low-voltage current to the semiconductor contacts (Figure S3 in the Supporting Information) does not influence the luminescence features of the indicator dye. The measured mean luminescence lifetime of the latter grafted to the LED chip surface is slightly lower than that obtained for the functionalized n-GaN (see above). Surprisingly enough, a p-GaN layer sits atop commercial LEDs and, therefore, no photoinduced charge-transfer deactivation of the indicator dye is to be expected. It must be taken into account that the LED p-GaN layer is usually covered by a very thin metallic p contact that is presumably removed during the plasma attack.[55] Should the metal layer not be completely eliminated, the subsequent grafting might place some ruthenium(II) dye molecules close enough to the metal islands, provoking a metal-enhanced emission effect via acceleration of the radiative deactivation rate.[56] Further studies are in progress on the novel functionalized devices to fully understand the photochemistry involved at the LED surface.

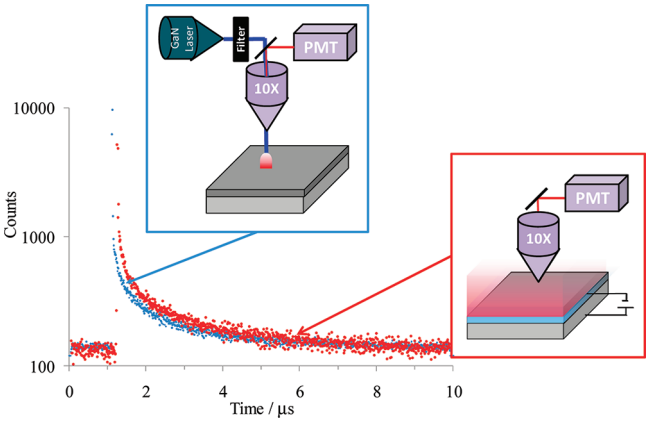

Figure 7. Luminescence emission decays under argon of a covalently functionalized GaN LED interrogated with an external picosecond laser (blue dots; λ_{exc} = 463 nm) and interrogated with the LED itself (red dots; λ_{em} > 590 nm).

4. CONCLUSIONS

GaN semiconductors can be successfully functionalized for chemical microsensing applications by covalent attachment of luminescent indicator dyes using oxygen plasma. The p-GaN surface rather than the n-GaN surface is required for fabrication of the sensitive device if the photoexcited grafted molecular probe is reducing enough to transfer an electron to the semiconductor conduction band. However, this charge injection process might be essential to develop the so-far-unknown DSSCs based on directly functionalized nitride semiconductors.

Integrateable microsensors based on luminescent indicators grafted to GaN might be the key step to realization of the *cell-phone-as-sensor* concept for in situ gas analysis in fields such as personal safety in home/work risk situations. The computational power of current smartphones is more than enough to analyze the optical signal and extract the emission lifetime information needed to determine an analyte concentration. Further studies on the way of tethering nanostructured GaN to indicator dyes should lead to a higher sensitivity of the resulting material to the analyte. All of these avenues are currently being explored in our laboratory for carbon monoxide, ethyl alcohol, and hydrogen sulfide gas sensing with GaN-based microdevices.

Table 1. Lifetime Values (under Argon) Obtained from the Fitting of the Luminescence Decays of the Functionalized LED Chip Recorded with an External Laser or the Functionalized LED Excitation[a]

excitation source	τ_1 (ns)	B_1 (%)	τ_2 (ns)	B_2 (%)	τ_3 (ns)	B_3 (%)	τ_m (ns) [d]
laser diode [b]	81	994 (54)	394	626 (33)	1855	160 (11)	**407**
LED [c]	60	901 (61)	396	415 (28)	2385	233 (13)	**415**

[a] $I(t) = A + \Sigma_i B_i e^{-t/\tau_i}$. [b] Estimated maximum uncertainty: 7% for τ_1, 8% for τ_2, 7% for τ_3, and 3% for τ_m. [c] Estimated maximum uncertainty: 18% for τ_1, 15% for τ_2, 8% for τ_3, and 4% for τ_m. [d] $\tau_m = \Sigma_i[(\%)_i/100]\tau_i$.

■ ASSOCIATED CONTENT

Supporting Information. Luminescence decays, emission lifetimes, and an instrument diagram for LED interrogation. This material is available free of charge via the Internet at http://pubs.acs.org.

■ AUTHOR INFORMATION

Corresponding Author
*Phone: +34 913 944 220. Fax: +34 913 944 103. E-mail: orellana@quim.ucm.es.

■ ACKNOWLEDGMENT

We thank Dr. Peter Parbrook, Dr. Tao Wang, and Dr. Fabio Ranalli from the University of Sheffield and EPSRC National Centre for III−V Technologies for the growth of the p-GaN samples. This project has been funded by the Spanish MICINN (Grant CTQ2009-14565-C03-01) and the UCM—Santander (Grant GR35/10-A).

■ REFERENCES

(1) Ryhänen, T., Uusitalo, M. A., Ikkala, O., Kärkkäinen, A., Eds. *Nanotechnologies for Future Mobile Devices*; Cambridge University Press: Cambridge, U.K., 2010.
(2) Krishna, S.; Boren, S. A.; Balas, E. A. *Telemed. J. e-Health* **2009**, *15*, 231–240.
(3) Lee, H. J.; Ha, R.; Jung, Y.; Lee, W. Health Management System and Method Using Mobile Phone. U.S. Patent Appl. 20090157429.
(4) Wang, S. X.; Zhou, X. J. Spectroscopic Sensor on Mobile Phone. U.S. Patent 7,420,663, Sept 2, 2008.
(5) Narayanaswamy, R., Wolfbeis, O. S., Eds. *Optical Sensors: Industrial, Environmental and Diagnostic Applications*; Springer Series on Chemical Sensors and Biosensors 1; Springer: Berlin, 2004.
(6) Rae, B. R.; Yang, J.; McKendry, J.; Gong, Z.; Renshaw, D.; Girkin, J. M.; Gu, E.; Dawson, M. D.; Henderson, R. K. *IEEE Trans. Biomed. Circuits Syst.* **2010**, *4*, 437–444.
(7) Vinogradov, S. A.; Fernandez-Searra, M. A.; Dugan, B. W.; Wilson, D. F. *Rev. Sci. Instrum.* **2001**, *72*, 3396–3406.
(8) Arranz, A.; Palacio, C.; García-Fresnadillo, D.; Orellana, G.; Navarro, A.; Muñoz, E. *Langmuir* **2008**, *24*, 8667–8671.
(9) López-Gejo, J.; Arranz, A.; Navarro, A.; Palacio, C.; Muñoz, E.; Orellana, G. *J. Am. Chem. Soc.* **2010**, *132*, 1746–1747.
(10) Cho, H. K.; Jang, J.; Choi, J.-H.; Choi, J.; Kim, J.; Lee, J. S. *Opt. Express* **2006**, *14*, 8654–8660.
(11) Piprek, J., Ed. *Nitride Semiconductor Devices*; Wiley-VCH: Weinheim, Germany, 2007.
(12) Chang, C. Y.; Kang, B. S.; Wang, H. T.; Ren, F.; Wang, Y. L.; Pearton, S. J.; Dennis, D. M.; Johnson, J. W.; Rajagopal, P.; Roberts, J. C.; Piner, E. L.; Linthicum, K. J. *Appl. Phys. Lett.* **2008**, *92*, 232102.
(13) Xu, X.; Jindal, V.; Shahedipour-Sandvik, F.; Bergkvist, M.; Cady, N. C. *Appl. Surf. Sci.* **2009**, *255*, 5905–5909.
(14) Estephan, E.; Larroque, C.; Cuisinier, F. J. G.; Bálint, Z.; Gergely, C. *J. Phys. Chem. B* **2008**, *112*, 8799–8805.
(15) Fahrenkopf, N. M.; Shahedipour-Sandvik, F.; Tokranova, N.; Bergkvist, M.; Cady, N. C. *J. Biotechnol.* **2010**, *15*, 312–314.
(16) Guo, D. J.; Abdulagatov, A. I.; Rourke, D. M.; Bertness, K. A.; George, S. M.; Lee, Y. C.; Tan, W. *Langmuir* **2010**, *26*, 18382–18391.
(17) Chu, B. H.; Kang, B. S.; Chang, C. Y.; Ren, F.; Goh, A.; Sciullo, A.; Wu, W.; Lin, J.; Gila, B. P.; Pearton, S. J.; Johnson, J. W.; Piner, E. L.; Linthicum, K. J. *IEEE Sens. J.* **2010**, *10*, 64–70.
(18) Uhlrich, J.; Garcia, M.; Wolter, S.; Brown, A. S.; Kuec, T. F. *J. Cryst. Growth* **2007**, *300*, 204–211.
(19) Kim, H.; Colavita, P. E.; Metz, K. M.; Nichols, B. M.; Sun, B.; Uhlrich, J.; Wang, X.; Kuech, T. F.; Hamers, R. J. *Langmuir* **2006**, *22*, 8121–8126.
(20) Linkohr, S.; Schwarz, S.; Krischok, S.; Lorenz, P.; Cimalla, V.; Nebel, C.; Ambacher, O. *Phys. Status Solidi C* **2010**, *7*, 1810–1813.
(21) Kim, H.; Colavita, P. E.; Paopraser, P.; Gopalan, P.; Kuech, T. F.; Hamers, R. J. *Surf. Sci.* **2008**, *602*, 2382–2388.
(22) Ganguly, A.; Chen, C.-P.; Lai, Y.-T.; Kuo, C.-C.; Hsu, C.-W.; Chen, K.-H.; Chen, L.-C. *J. Mater. Chem.* **2009**, *19*, 928–933.
(23) Petoral, R. M., Jr.; Yazdi, G. R.; Lloyd Spetz, A.; Yakimova, R.; Uvdal, K. *Appl. Phys. Lett.* **2007**, *90*, 223904.
(24) Yakimova, R.; Steinhoff, G.; Petoral, R. M., Jr.; Vahlberg, C.; Khranovskyy, V.; Yazdi, G. R.; Uvdal, K.; Lloyd Spetz, A. *Biosens. Bioelectron.* **2007**, *22*, 2780–2785.
(25) Baur, B.; Steinhoff, G.; Hernando, J.; Purrucker, O.; Tanaka, M.; Nickel, B.; Stutzmann, M.; Eickhoff, M. *Appl. Phys. Lett.* **2005**, *87*, 263901.
(26) Kang, B. S.; Ren, F.; Wang, L.; Lofton, C.; Tan, W. W.; Peartona, S. J.; Dabiran, A.; Osinsky, A.; Chow, P. P. *Appl. Phys. Lett.* **2005**, *87*, 023508.
(27) Ismail, M. N.; Goodrich, T. L.; Ji, Z.; Ziemer, K. S.; Warzywoda, J.; Sacco, A., Jr. *Microporous Mesoporous Mater.* **2009**, *118*, 245–250.
(28) Simpkins, B. S.; McCoy, K. M.; Whitman, L. J.; Pehrsson, P. E. *Nanotechnology* **2007**, *18*, 355301.
(29) Fang, D. Q.; Rosa, A. L.; Frauenheim, T.; Zhang, R. Q. *Appl. Phys. Lett.* **2009**, *94*, 073116.
(30) Hsu, C.-W.; Ganguly, A.; Chen, C.-P.; Kuo, C.-C.; Paskov, P. P.; Holtz, P. O.; Chen, L.-C.; Chen, K.-H. *J. Appl. Phys.* **2011**, *109*, 053523.
(31) Magalhães, S.; Peres, M.; Fellmann, V.; Daudin, B.; Neves, A. J.; Alves, E.; Monteiro, T.; Lorenz, K. *J. Appl. Phys.* **2010**, *108*, 084306.
(32) Orellana, G.; García-Fresnadillo, D. In *Optical Sensors: Industrial, Environmental and Diagnostic Applications*; Narayanaswamy, R., Wolfbeis, O. S., Eds.; Springer Series on Chemical Sensors and Biosensors; Springer: Berlin, 2004; Vol. 1, p 309.
(33) Chu, B. W.-K.; Yam, V. W.-W. *Langmuir* **2006**, *22*, 7437–7443.
(34) Lei, B.; Li, B.; Zhang, H.; Lu, S.; Zheng, Z.; Li, W.; Wang, Y. *Adv. Funct. Mater.* **2006**, *16*, 1883–1891.
(35) Lupo, F.; Fragala, M. E.; Gupta, T.; Mamo, A.; Aureliano, A.; Bettinelli, M.; Speghini, A.; Gulino, A. *J. Phys. Chem. C* **2010**, *114*, 13459–13464.
(36) Xavier, M. P.; García-Fresnadillo, D.; Moreno-Bondi, M. C.; Orellana, G. *Anal. Chem.* **1998**, *70*, 5184–5189.
(37) Carraway, E. R.; Demas, J. N.; DeGraff, B. A. *Anal. Chem.* **1991**, *63*, 332–336.
(38) Stein, R.; Simpkins, B. S.; Mulvaney, S. P.; Whitman, L. J.; Tamanaha, C. R. *Appl. Surf. Sci.* **2010**, *256*, 4171–4175.
(39) Stine, R.; Cole, C. L.; Ainslie, K. M.; Mulvaney, S. P.; Whitma, L. J. *Langmuir* **2007**, *23*, 4400–4404.
(40) García-Fresnadillo, D.; Orellana, G. *Helv. Chim. Acta* **2001**, *84*, 2708–2730.
(41) Alford, P. C.; Cook, M. J.; Lewis, A. P.; McAuliffe, G. S. G.; Skarda, V.; Thomson, A. J. *J. Chem. Soc., Perkin Trans. 2* **1985**, 705–709.
(42) Xia, H.; Li, M.; Lu, D.; Zhang, C.; Xie, W.; Liu, X.; Yang, B.; Ma, Y. *Adv. Funct. Mater.* **2007**, *17*, 1757–1764.
(43) López-Gejo, J.; Haigh, D.; Orellana, G. *Langmuir* **2010**, *26*, 2144–2150.
(44) Campagna, S.; Puntoriero, F.; Nastasi, F.; Bergamini, G.; Balzani, V. *Top. Curr. Chem.* **2007**, *280*, 117–214.
(45) Beach, J. D.; Collins, R. T.; Turner, J. A. *J. Electrochem. Soc.* **2003**, *150*, A899–A904.
(46) Zanarini, S.; Ciana, L. D.; Marcaccio, M.; Marzocchi, E.; Paolucci, F.; Prodi, L. *J. Phys. Chem. B* **2008**, *112*, 10188–10193.
(47) Howgate, J.; Schoell, S. J.; Hoeb, M.; Steins, W.; Baur, B.; Hertrich, S.; Nickel, B.; Sharp, I. D.; Stutzmann, M.; Eickhoff, M. *Adv. Mater.* **2010**, *22*, 2632–2636.
(48) Chen, X. Y.; Yip, C. T.; Fung, M. K.; Djurišić, A. B. *Appl. Phys. A: Mater. Sci. Process.* **2010**, *100*, 15–19.
(49) Zywietz, T. K.; Neugebauer, J.; Scheffler, M. *Appl. Phys. Lett.* **1999**, *74*, 1695–1697.
(50) McGee, K. A.; Mann, K. R. *J. Am. Chem. Soc.* **2009**, *131*, 1896–1902.

(51) Mingoarranz, F. J.; Moreno-Bondi, M. C.; García-Fresnadillo, D.; de Dios, C.; Orellana, G. *Microchim. Acta* **1995**, *121*, 107–118.
(52) Orellana, G.; Moreno-Bondi, M. C.; Garcia-Fresnadillo, D.; Marazuela, M. D. In *Chemical Sensors: Novel Principles and Techniques*; Orellana, G., Moreno-Bondi, M. C., Eds.; Springer Series on Chemical Sensors and Biosensors; Springer: Berlin, 2005; Vol. 3, p 189.
(53) Reshchikova, M. A.; Morkoç, H. *J. Appl. Phys.* **2005**, *97*, 061301.
(54) Molnar, R. J. In *Gallium Nitride (GaN) II, Semiconductors and Semimetals*; Pankove, J. I., Moustakas, T. D., Eds.; Academic Press: New York, 1990.
(55) Morkoç, H., Ed. *Handbook of Nitride Semiconductors and Devices, Vol. 2: Electronic and Optical Processes in Nitrides*; Wiley-VCH: Weinheim, Germany, 2009.
(56) Lakowicz, J. R., Geddes, C. D., Eds. *Topics in Fluorescence Spectroscopy, Vol. 8: Radiative Decay Engineering*; Springer: New York, 2009.